

## Process optimization and kinetic evaluation of Amberlite IR 120 and sulphamic acid catalyzed esterification of acetic acid and methanol

Rajeev Kumar Dohare\*<sup>a</sup>, Abhishek Srivastava<sup>b</sup> & Parvez Ansari<sup>a</sup>

<sup>a</sup>Department of Chemical Engineering, Malaviya National Institute of Technology, Jaipur 302 017, Rajasthan, India

<sup>b</sup>Department of Chemistry, GLA University, Mathura 281 406, Uttar Pradesh, India

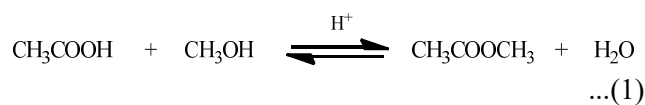
E-mail: rkdohare.chem@mnit.ac.in

Received 21 December 2023; accepted (revised) 27 June 2024

The Box-Behnken design-based Response Surface Methodology (RSM) has been effectively utilized to optimize the parameters for operation in the amberlite IR 120 and sulphamic acid-catalyzed esterification of methanol and acetic acid. The impact of three process variables, temperature, catalyst loading, and the mole ratio of methanol to acetic acid on esterification has been evaluated. The esterification process exhibits excellent concordance between the predicted values and the experimental values ( $R^2 = 98.33\%$  and  $\text{Adj-}R^2 = 92.08\%$ ), which indicate the suitability of the Box-Behnken model employed. The interaction of the parameters is also studied based on its  $P$ -value with the help of ANOVA variance. The second-order kinetic rate equation is applied to correlate the experimental data. By employing the Arrhenius graph, the rate constants for the backward ( $12.727 \times 10^8 \text{ lit mol}^{-1} \text{ min}^{-1}$ ) and forward reactions ( $2.324 \times 10^4 \text{ lit mol}^{-1} \text{ min}^{-1}$ ), as well as the energy of activation using amberlite IR 120, have been determined. The statistical methodologies, including factorial design and Box-Behnken response, have been employed to model the conversion of acetic acid using various regression techniques for a quadratic equation. The result shows that the amberlite IR 120 catalyst is better than the sulphamic acid catalyst due to the more active catalytic surface area.

**Keywords:** Box-Behnken model, Response surface methodology, Esterification, Ion exchange, Amberlite IR 120, Sulphamic Acid

The esterification reaction of acetic acid with methanol to produce methyl acetate and the backward reaction, methyl acetate hydrolysis, have growing interest in reactive distillation as a model reaction<sup>1,2</sup>. Esterification is the reaction in which the process of the ester is produced by combining alcohol and carboxylic acid<sup>3-8</sup>. The methyl acetate synthesis reaction scheme is given as:



The esterification forms methyl acetate in a reversible reaction process by using methanol and acetic acid and adding a catalyst. This reaction can be done in batch and continuous methods. This reaction is mainly used on a smaller scale in chemical laboratories. Methyl acetate is used in different applications, such as producing solvents, perfumes, biodiesel fuels, and surfactants<sup>9-13</sup>.

The better performance of homogenous acid catalysts shows that they have some challenging occurrences of side reactions and separation in

catalyst from product formation. Therefore, the catalyst types are heterogeneous like microporous solids, carbon/graphitic structures, and metal oxides<sup>14-18</sup>. The main constraints in the homogenous catalyst are higher cost and reaction disturbances that permit the use of a solid catalyst, which provides the catalyst separation steps and can be recycled. Therefore, the simultaneous reaction of methyl acetate synthesis is cheaper than another esterification process<sup>19</sup>. In the absence of a catalyst, the response takes more time to reach equilibrium. Using a catalyst increases the reaction rate to maintain the extent of the reaction.

The use of reactive distillation will separate methanol to methyl acetate and waste oils. For the implantation of the simulation technique for the waste collection process, kinetic data, as well as thermodynamic properties, are needed. Due to using a better catalyst, the kinetic data was fixed accordingly. Kinetic values are calculated over a similar composition type from the kinetic knowledge of methanol and acetic acid. The main aim of the research is to provide the kinetic data of methanol and acetic acid esterification reactions used on a single

batch reactor<sup>20</sup>. The reaction can be influenced by the inherent phase of the reaction, which can be altered through temperature modulation and pressure adjustments, thereby modifying the properties of the reactants. These results can be attributed to the lack of expensive enzymes, noxious solvents, or catalysts that typically yield the production of methyl acetate synthesis for subsequent application<sup>21</sup>. Homogeneous catalysts for the esterification of the mineral acid used are HCl, HBr, HI, and H<sub>2</sub>SO<sub>4</sub>. Heterogeneous catalysts exhibit superior performance compared to homogeneous catalysts owing to their versatile applications, such as facilitating the reduction of corrosive environments<sup>8</sup>. The trial runs have been done at a temperature range of 308.15 K to close to its bubble point temperature range of reaction and the molar ratio such as 1:1 and 1:3.

Esterification process variables have been optimized using different statistically constructed experimental models. To investigate the influence of process factors, classic optimization experiments varied one variable while maintaining the other constant. Experimental design approaches can maximize effective parameters with fewer experiments. Response surface methodology (RSM) is a mathematical and statistical approach for planning experiments, generating models, assessing independent variable significance, and establishing optimal response conditions<sup>22</sup>. RSM determines optimal operating conditions at a certain operational specification, not a system mechanism. Complex system performance has been optimized and understood using it<sup>23,24</sup>. RSM evaluates interactions between tested operational factors and reduces experimentation for an equal number of estimated variables compared to the traditional technique. Numerous esterification procedures have been modelled and optimized using RSM<sup>25-31</sup>.

The principal objective of this investigation is to elucidate the functional relationship between key parameters governing the esterification process (catalyst concentration, initial molar ratio of reactant, and reaction temperature) and their influence on the transformation of acetic acid or the formation of the resultant product. The utilization of Box-Behnken design coupled with response surface methodology was elucidated to establish a correlation between the independent variables and the resultant output response (transformation of acetic acid). The optimum operating conditions for the esterification of methanol and acetic acid, catalyzed by amberlite IR 120 and sulphamic acid, were successfully determined.

## Experimental Section

### Reagents used

All experiment was conducted using double-deionized water and analytical grade reagents over the entire study. Methanol utilized (Finar Chemicals Ltd. Mumbai, India) was of utmost purity. Merck Life Science Pvt Ltd (Mumbai, India) supplied acetic acid (99.95%). Amberlite IR 120 catalyst purchased from Research lab (Mumbai, India), and sulphamic acid (Rankem, Gurgaon, India) was utilized without subsequent purification.

### Procedure for methyl acetate synthesis

The acetic acid and methanol were mixed in the three-neck flask, with their respective measured quantities. The stoichiometric quantities of the pristine liquid reactants have been equilibrated using an electronic balance with a precision of  $\pm 0.001$ g. The reaction mixture exhibits pronounced reactivity at the selected reaction temperatures (308.15K, 318.15K, 328.15 K, 330.15 K, and 333.15 K). For the selected chemical transformation, the catalyst plays a crucial role, while the temperature serves as a supplementary factor within the optimal reaction parameters. The sample was taken during the reaction so that it could be titrated to find out the composition of product.

The samples were extracted at precise time interval of 5 minutes, subjected to titration using standard NaOH solution, and the concentration of the resulting product was determined through gas chromatography analysis. Upon increasing the molar ratio of the reactant to catalyst, the equilibrium is rapidly attained.

### Experimental setup

The esterification reaction between methanol and acetic acid was conducted within a 1000 ml 3-necked round bottom flask, commonly referred to as a Dean Stark apparatus. The reaction mixture was subjected to agitation using a hotplate magnetic stirrer, with stirring speeds ranging from 230 rpm to 600 rpm to ensure effective mixing. A mercury-filled thermometric device was employed to determine the temperature of the reaction medium within. A condenser has been positioned within the 3-necked round-bottom flask to facilitate the condensation of vapours, which subsequently reintegrate into the reaction mixture. The schematic and experimental arrangement is depicted in Fig. 1.

### Optimization design

The Response Surface Methodology (RSM) technique is a collection of mathematical and statistical techniques employed for the purpose of optimization. Its primary aim is to optimize the response, which is influenced by various factors, by determining the optimal values at which the desired response is achieved. The mathematical and statistical design of various experiments entails the utilization of

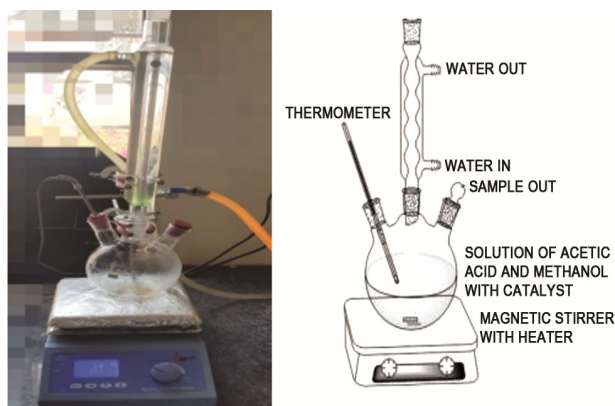


Fig. 1 — Experimental setup for the esterification of acetic acid and methanol

methodologies to optimize response surfaces and minimize the quantity of conducted experiments. It facilitated the modelling of the response system, which is contingent upon various variables<sup>17</sup>. The synthesis of methyl acetate utilizing methanol and acetic acid was conducted, and the associated parameters were investigated using RSM in MINITAB 19 software.

Tables 1 and 2 exhibit the factorial design elucidating the conversion of acetic acid through the utilization of sulphamic acid and amberlite IR 120, correspondingly. The data demonstrates the F-value and *P*-value, wherein a smaller *P*-value indicates a more significant response, while a larger *P*-value indicates a less significant response. The model summary of the factorial design is presented in Table 3, wherein the R-square value for the sulphamic acid catalyst is observed to be 98.33%, while for the amberlite IR 120 catalyst, it is found to be 99.52%.

The generated factorial plots (Fig. S1 and Fig. S2) from the Minitab software elucidating the diverse parameters encompassing temperature, molar ratio, and catalyst loading for sulphamic acid and amberlite IR 120, respectively. The Pareto chart reveals the

Table 1 — Analysis of variance (factorial design) for sulphamic acid catalyst

Source	DF	Adj SS	Adj MS	F-Value	P-Value
Model	15	3594.33	239.622	15.74	0.008
Linear	6	3498.71	583.119	38.29	0.002
Temperature	4	2620.64	655.160	43.03	0.002
Molar Ratio	1	640.71	640.712	42.08	0.003
Catalyst	1	237.36	237.360	15.59	0.017
2-Way Interactions	9	95.61	10.624	0.70	0.701
Temperature*Molar Ratio	4	75.42	18.854	1.24	0.420
Temperature*Catalyst	4	17.87	4.468	0.29	0.869
Molar Ratio*Catalyst	1	2.33	2.326	0.15	0.716
Error	4	60.91	15.227		
Total	19	3655.23			

Table 2 — Analysis of variance (factorial design) for amberlite IR-120 catalyst

Source	DF	Adj SS	Adj MS	F-Value	P-Value
Model	15	2682.48	178.832	55.75	0.001
Linear	6	2526.55	421.091	131.28	0.000
Temperature	4	1571.78	392.946	122.50	0.000
Molar Ratio	1	639.47	639.467	199.35	0.000
Catalyst	1	315.30	315.297	98.29	0.001
2-Way Interactions	9	155.93	17.326	5.40	0.060
Temperature*Molar Ratio	4	142.58	35.644	11.11	0.019
Temperature*Catalyst	4	12.22	3.056	0.95	0.518
Molar Ratio*Catalyst	1	1.14	1.138	0.35	0.584
Error	4	12.83	3.208		
Total	19	2695.31			

heightened stability of all factors pertaining to the conversion of acetic acid.

Each variable employed in the provided experiment has been coded as levels +1, 0, and -1, as illustrated in Table 4 (pertaining to sulphamic acid) and Table 5 (pertaining to amberlite IR 120). These tables represent the Box-Behnken design encompassing all three factors expressed in coded units.

The preliminary data presented in Table 6 (sulphamic acid) and Table 7 (amberlite IR 120) was scrutinized utilizing the response surface methodology (RSM). The RSM for the conversion of acetic acid was designed using MINITAB 19 software, incorporating various parameters such as temperature, molar ratio of reactants, and catalyst loading. The analysis of variance (ANOVA) was employed to determine the significance of these factors.

Table 3 — Model Summary

	S	R <sup>2</sup>	R <sup>2</sup> (adj)	R <sup>2</sup> (pred)
Sulphamic acid	3.90222	98.33%	92.08%	58.34%
Amberlite IR-120	1.79100	99.25%	97.74%	88.10%

Table 4 — Box Behnken experiment design (for sulphamic acid)

Run	Blk	A	B	C
1	1	-1	-1	0
2	1	1	-1	0
3	1	-1	1	0
4	1	1	1	0
5	1	-1	0	-1
6	1	1	0	-1
7	1	-1	0	1
8	1	1	0	1
9	1	0	-1	-1
10	1	0	1	-1
11	1	0	-1	1
12	1	0	1	1
13	1	0	0	0
14	1	0	0	0
15	1	0	0	0

Table 6 — Estimated regression coefficient, t and p-value of Box-Behnken design (for sulphamic acid)

Term	Coef	SE Coef	T-Value	P-Value	VIF
Constant	59.02	2.93	20.13	0.000	
Temperature	14.17	1.80	7.89	0.001	1.00
Catalyst	4.25	1.80	2.36	0.064	1.00
Molar Ratio	3.10	1.80	1.72	0.145	1.00
Temperature*Temperature	-0.94	2.64	-0.36	0.736	1.01
Catalyst*Catalyst	-2.32	2.64	-0.88	0.420	1.01
Molar Ratio*Molar Ratio	1.49	2.64	0.57	0.596	1.01
Temperature*Catalyst	-1.48	2.54	-0.58	0.584	1.00
Temperature*Molar Ratio	3.22	2.54	1.27	0.261	1.00
Catalyst*Molar Ratio	0.25	2.54	0.10	0.924	1.00

Tables 1 and 2 present the computed t-values and p-values for each of the individual terms. The null hypothesis postulates that the factor coefficient has a value of zero, provided that the t-value exceeds that of every parameter. Consequently, the critical t-value refutes the null hypothesis for the specified response. The p-value elucidated the statistical significance of the observed response. If the p-value attains the minimum value, the significance of the regression coefficient is heightened. Tables 6 and 7 present the regression coefficient, p-value, and t-value obtained from the Box-Behnken design. Additionally, Table 8 provides the model summary based on the Box-Behnken design optimization technique. Table 8 shows the summary Table of R-square values which reveals that R-square (pred) has 0.0% value in case of both catalyst but R-Sq and R-Sq(adj) values are higher in the case of IR 120 catalyst *i.e.* 96.95% and 86.47% respectively, in comparison to the Sulphamic acid catalyst. Based on the R-square values it could be concluded that the model is best fit for the IR-120 catalyst.

Table 5 — Box Behnken experiment design (for amberlite IR-120)

Run	Blk	A	B	C
1	1	0	1	1
2	1	0	-1	-1
3	1	-1	0	1
4	1	-1	-1	0
5	1	1	-1	0
6	1	0	0	0
7	1	0	1	-1
8	1	-1	0	-1
9	1	-1	1	0
10	1	0	0	0
11	1	1	1	0
12	1	0	-1	1
13	1	1	0	1
14	1	0	0	0
15	1	1	0	-1

Table 7 — Estimated regression coefficient, t and p value of Box-Behnken design (for amberlite IR-120)

Term	Coef	SE Coef	T-Value	P-Value	VIF
Constant	62.67	2.19	28.66	0.000	
Temperature	12.42	1.34	9.27	0.000	1.00
Catalyst	2.97	1.34	2.22	0.078	1.00
Molar Ratio	4.97	1.34	3.71	0.014	1.00
Temperature*Temperature	-1.00	1.97	-0.50	0.635	1.01
Catalyst*Catalyst	1.71	1.97	0.87	0.426	1.01
Molar Ratio*Molar Ratio	1.30	1.97	0.66	0.538	1.01
Temperature*Catalyst	-4.51	1.89	-2.38	0.063	1.00
Temperature*Molar Ratio	2.47	1.89	1.31	0.248	1.00

Table 8 — Model Summary of Box- Behnken design

	S	R <sup>2</sup>	R <sup>2</sup> (adj)	R <sup>2</sup> (pred)
Sulphamic acid	5.07801	93.68%	82.29%	0.00%
Amberlite IR-120	1.9672	97.95%	86.47%	0.00%

Amberlite IR-120 shows higher R-square values *i.e.* 97.95%, concerning to the sulphamic acid catalyst as envisaged in Table 8. It reveals that for the IR-120 is a best-fit model to predict the optimum conversion of the esterification reaction.

The 3D plots depicting the response and contours can be represented as a function of variables, including molar ratio *versus* temperature, catalyst *versus* temperature, and molar ratio *versus* catalyst. These relationships are illustrated in Fig. S3 (sulphamic acid) and Fig. S4 (amberlite IR 120). The graph was plotted by varying two independent variables while maintaining a constant value for a third variable. The discernible influence of the molar ratio of reactants in relation to the reaction temperature becomes evident when the catalyst loading is maintained at 4%.

## Results and Discussion

### Esterification analysis

The investigation involves the examination of the reaction between methanol and acetic acid, facilitated by a catalyst, to produce methyl acetate. Various parameters are being explored, including the mole ratio of reactants ranging from 1:1 to 1:3, the temperature spanning from 308.15 K to 333.15 K, and the catalyst loading varying between 3% and 5% (depending on the initial molar ratio of reactants). The speed of the magnetic stirrer changes from 230 rpm to 600 rpm.

### Effect of sulphamic acid

#### Effect of reaction temperature

In the feed solution comprising methanol and acetic acid in a molar ratio of 1:1, the observed

conversions of acetic acid were measured at various temperatures. The data indicates that as the temperature of the solution is raised from 308.15 K to 333.15 K, the conversion of acetic acid increases from 24.46% to 62.66%. These results were obtained under different experimental conditions, as depicted in Fig. 2.

### Effect of Catalyst Loading

The temporal transformation of acetic acid has been investigated under experimental parameters including reaction temperature, mole ratio in relation to catalyst loading, and agitation speed, alongside model forecasts based on adsorption-based models. It is evident that the acetic acid conversion exhibits an upward trend as the catalyst loading escalates from 3% to 5%. The percentage conversion of acetic acid ranges from 62.44% to 66.13%. The graph depicting the loading of the catalyst is illustrated in Fig. 3.

### Effect of initial reactants mole ratio

The temporal dependence of the transformation rate of acetic acid is contingent upon the influence exerted by the initial molar ratio. The molar ratio of acetic acid to methanol in the experimental scenarios varied from 1:1 to 1:3, with catalyst quantity of 3%. The reactions were conducted at a temperature of 333.15 K and a stirring rate of 240 rpm. With the progressive augmentation of the molar ratio of acetic acid to methanol within the range of 1:1 to 1:3, the percentage of conversion of acetic acid experienced an upward trend, escalating from 62.66% to 70.10% as depicted in Fig. 4.

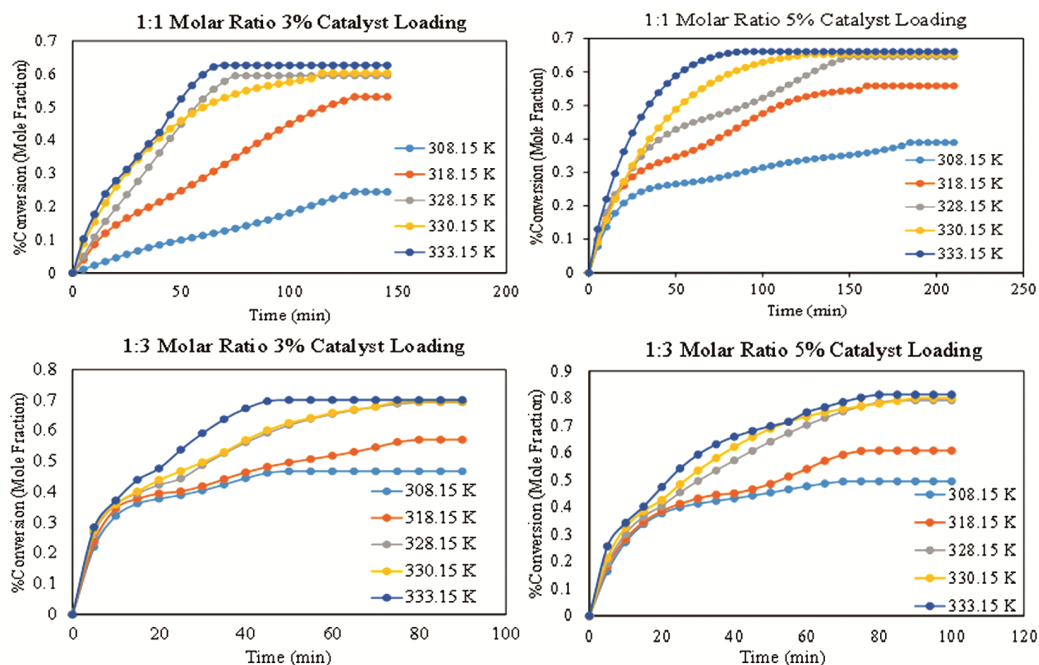


Fig. 2 — Percentage conversion of acetic acid using sulphamic acid at different temperatures

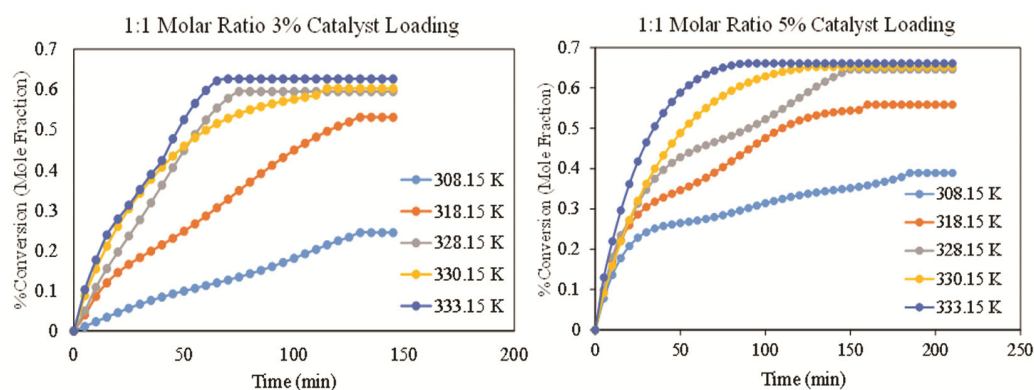


Fig. 3 — Percentage conversion of acetic acid using sulphamic acid at different catalyst loading

### Amberlite IR 120 Catalyst

The investigation of the catalytic esterification between acetic acid and methanol in the presence of Amberlite IR 120 was conducted using mole ratios ranging from 1:1 to 1:3. The temperature of the reaction has exhibited fluctuations within the range of 308.15 K to 333.15 K, while the loading of the catalyst has undergone alterations ranging from 3% to 5% relative to the initial composition of the reaction mixture.

### Effect of Reaction Temperature

Acetic acid conversion was achieved at varying temperatures with a set catalyst loading of 3 and 5%, and an agitation speed of 240 rpm, at fixed molar

ratios of reactants of 1:1 and 1:3. The findings from the experiment indicate that the conversion of acetic acid exhibits an upward trend, reaching 42.92% at a temperature of 308.15 K and 63.37% at 333.15 K. These results pertain to a reaction conducted with a 1:1 molar ratio and a catalyst loading of 3%, as depicted in Fig. 5.

### Effect of Catalyst Loading

The temporal investigation of acetic acid conversion has been conducted under experimental parameters encompassing reaction temperature, mole ratio of reactants, and agitation speed. The experimental findings indicate that the acetic acid conversion exhibits an upward trend as the catalyst loading is augmented,

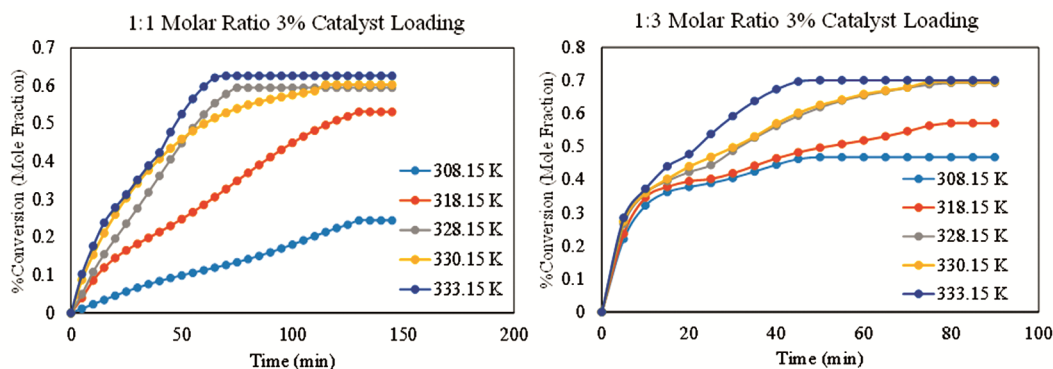


Fig. 4 — Percentage conversion of acetic acid using sulphamic acid at different molar ratios

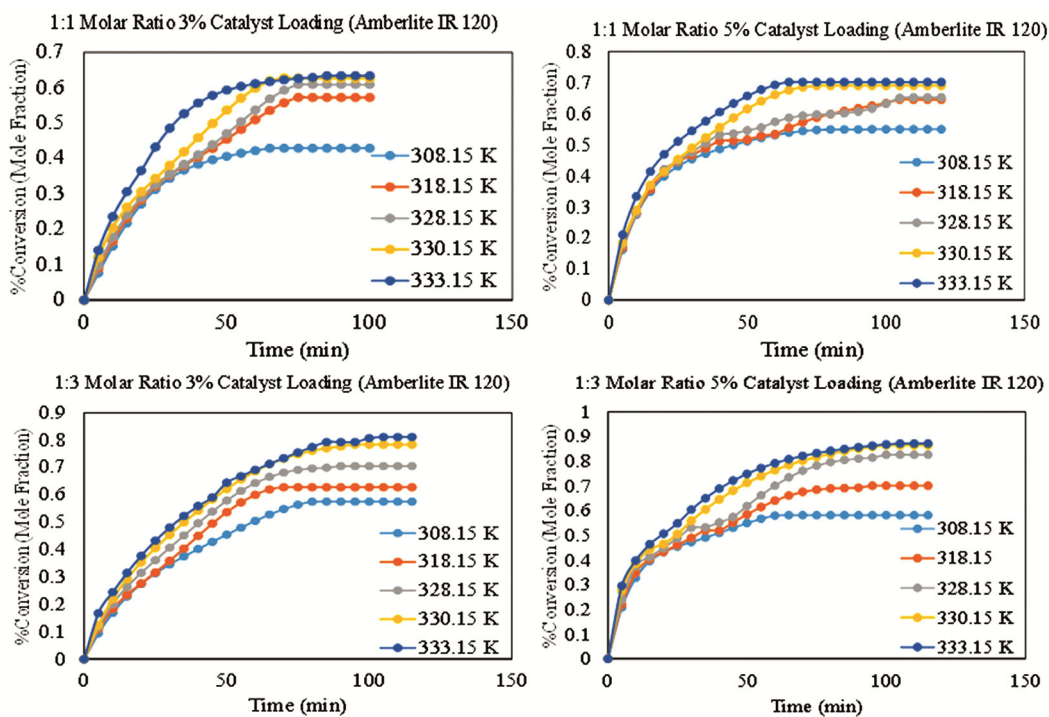


Fig. 5 — Percentage conversion of acetic acid using amberlite IR 120 at different temperatures

ranging from 63.33% to 70.10% for catalyst loadings of 3% and 5% respectively, while maintaining a constant temperature of 333.15 K and a molar ratio of 1:1. The observed augmentation can be attributed to the enhanced surface area of the active catalyst, resulting in an amplified reaction composition and a subsequent escalation in the reaction rate, as depicted in Fig. 6.

### Effect of Initial Reactant Mole Ratio

Initial molar ratio of reactants had an impact on the rate at which acetic acid converted to time. With catalyst amounts of  $0.03 \text{ g cm}^{-3}$ , temperature of 333.15 K, and agitation speed of 240 rpm, the initial molar ratio of acetic acid to methanol

varied between 1:1 and 1:3. The outcome demonstrates that acetic acid conversion rises as the mole ratio grows. As Fig. 7 illustrates that the acetic acid conversion percentage increased from 63.37% to 81.11% when the molar ratio of acetic acid to methanol increased from a range of 1:1 to 1:3.

### Comparative Study graphs

The esterification reaction demonstrated a higher conversion of acetic acid when employing the Amberlite IR 120 catalyst, in contrast to the sulphamic acid and Amberlyst 36<sup>8</sup>, at a temperature of 333.15 K, as illustrated in Fig. 8.

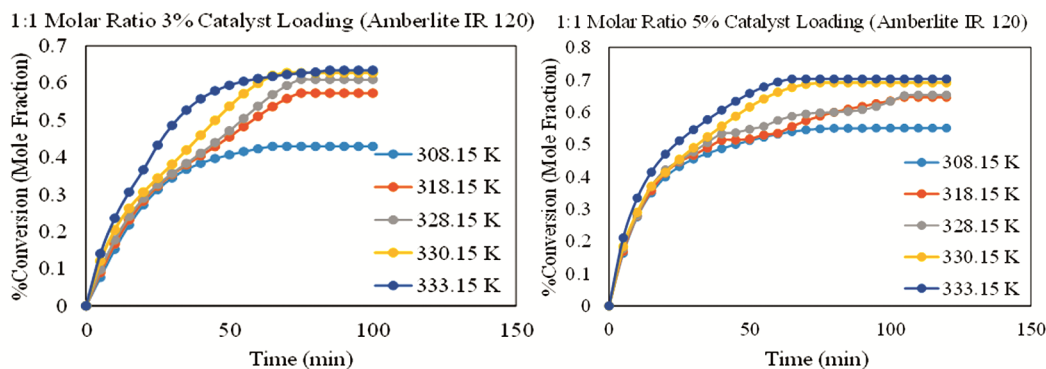


Fig. 6 — Percentage conversion of acetic acid using amberlite IR 120 at different catalyst loading

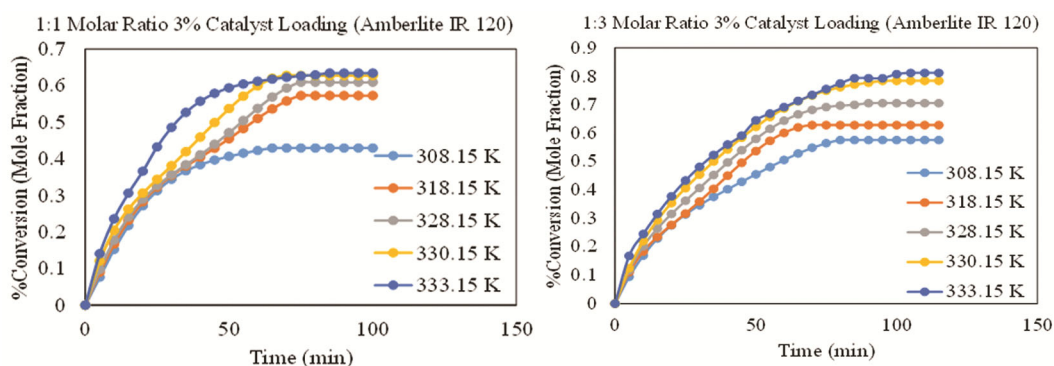


Fig. 7 — Percentage conversion of acetic acid using amberlite IR 120 at different molar ratio

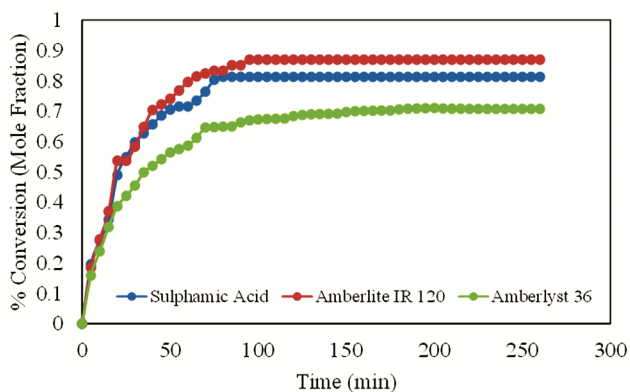


Fig. 8 — Comparative study of sulphamic acid and Amberlite IR 120

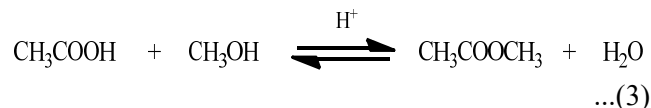
### Kinetic Modelling

The synthesis of methyl acetate is governed by a second-order reversible reaction. The Pseudo-Homogeneous (PH) model, also known as the Langmuir-Hinshelwood (LHW) model, is commonly characterized by its reliance on the ion-exchange resin model. The reaction yields methyl acetate and water as the product within the reactor, thus indicating that the pseudo-homogeneous model is adequate<sup>32</sup>.

Reaction:



A = Acetic Acid  
B = Methyl Alcohol  
C = Methyl Acetate  
D = Water



$$C_{A0} = C_{B0} \text{ and}$$

$$C_{C0} = C_{D0} = 0$$

The rate of the equation has been written as

$$-r_B = -\frac{dC_B}{dt} = C_{B0} \frac{dX_B}{dt} \quad \dots(4)$$

$$= k_1 C_A C_B - k_2 C_C C_D$$

$$= k_1 C_{B0}^2 (1 - X_B)^2 - k_2 (C_{B0} X_B)^2$$

$k_1$  = Rate constant of forward reaction

$k_2$  = Rate constant of backward reaction

At equilibrium,  $-r_B = 0$ .

So, the fractional transformation of B (methanol) under conditions of equilibrium is given by,

$$K_e = \frac{C_{Ce}C_{De}}{C_{Ae}C_{Be}} = \frac{X_{Be}^2}{(1-X_B)^2} \quad \dots(5)$$

The equilibrium constant of a reaction is given by,

$$K_e = \frac{k_1}{k_2} \quad \dots(6)$$

From all three above equations, in terms of equilibrium conversion, we get

$$\frac{dX_B}{dt} = k_1 C_{B0} \left[ (1-X_B)^2 - \left( \frac{1-X_{Be}^2}{X_{Be}} \right) X_B^2 \right] \quad \dots(7)$$

With the desired transformations in relation to  $X_{Be}$ , this can be represented as a pseudo-second-order reversible reaction, which, upon integration, yields the following equation,

$$\ln \left[ \frac{X_{Be} - (2X_{Be} - 1)X_B}{X_{Be} - X_B} \right] = 2k_1 \left( \frac{1}{X_{Be}} - 1 \right) C_{B0} t \quad \dots(8)$$

Through the utilization of Arrhenius law, the requisite temperature conditions for rate constants were ascertained.

$$k_1 = k_1^0 \exp \left( \frac{-E_1}{RT} \right) \quad \dots(9)$$

$$k_2 = k_2^0 \exp \left( \frac{-E_2}{RT} \right) \quad \dots(10)$$

An analysis of the plot of  $\ln k_1$  vs  $1/T$  yielded the activation energy of the reaction.

Where,

$K_e$  = equilibrium constant

$k_1^0$  and  $k_2^0$  = Arrhenius pre-exponential factors

$E_2$  = Activation energy of the backward reaction

$E_1$  = Activation energy of the forward reaction

A pseudo-homogenous model is employed to accurately describe the kinetics of the reaction under various conditions, such as catalyst loading, temperature variations, and mole ratio of the reactants.

### Kinetic parameters estimation using Amberlite IR 120 catalyst

The esterification reaction for the production of methyl acetate, involving methanol and acetic acid,

was conducted under kinetic operation conditions, as there were no interparticle diffusion resistance or external mass transfer resistance observed. Through the utilization amberlite IR 120 catalyst, the esterification reaction for the synthesis of methyl acetate was kinetically regulated. This process involved the combination of methanol and acetic acid in a stoichiometric ratio of 1:1, employing a catalyst loading of 3% (amberlite IR 120). The reaction was carried out within the temperature range of 308.15 K to 333.15 K, utilizing a stirred batch reactor. A pseudo-homogeneous kinetic model was employed to correlate the experimental data. The experimental data obtained within the temperature range of 308.15 K to 330.15 K were utilized to construct a graph based on the provided equation (9). The outcome of this analysis revealed a linear relationship between time and the observed values, with the line passing through the origin.

The gradients of the aforementioned lines on the graph correspond to the values of the forward reaction rate constant ( $k_1$ ), which were observed to be 0.006, 0.0074, 0.0076, and 0.0083 (l/mol.min) at temperatures of 308.15 K, 318.15 K, 328.15 K, and 330.15 K, respectively, as depicted in Fig. 9. By employing the  $k_1$  values within the Arrhenius equation, the  $-\ln k$  was plotted against  $1/T$  as depicted in Figure 10. The activation energy value obtained was 10.64, and 47.65 (kJ mol<sup>-1</sup>) for forward and backward reaction, respectively. The parameters estimated by the model are provided in Table 9.

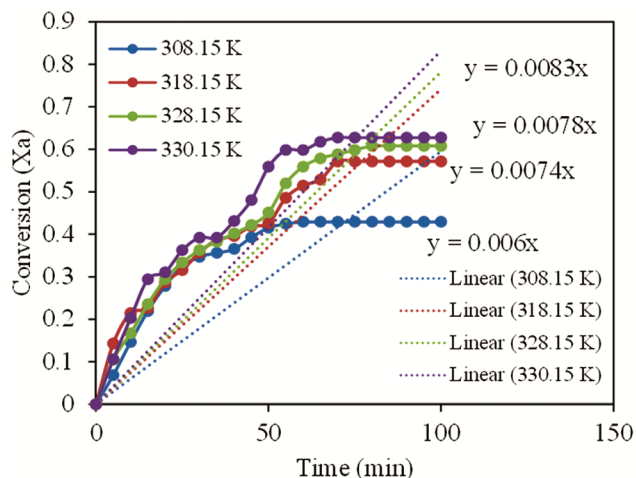


Fig. 9 — Determination of rate constants at different temperatures

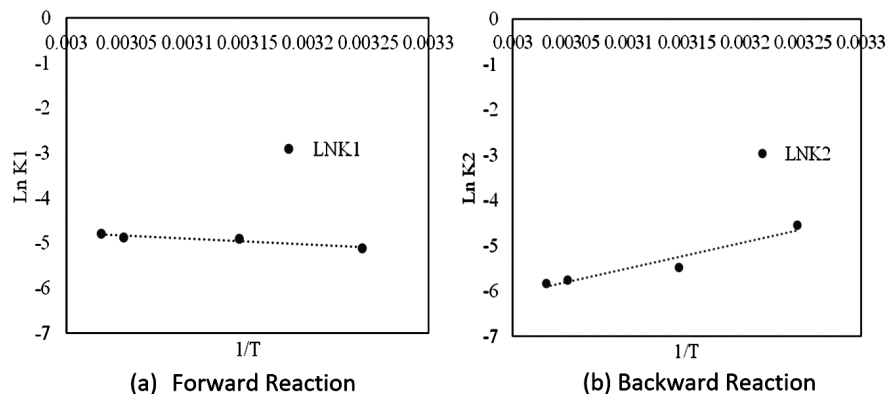


Fig. 10 — Arrhenius plot for reaction

Table 9 — Estimated results of kinetic data for esterification using amberlite IR 120

Parameters	Values
$E_1$ (kJ mol <sup>-1</sup> )	10.64
$E_2$ (kJ mol <sup>-1</sup> )	47.65
$k_1^0$ (lit mol <sup>-1</sup> min <sup>-1</sup> )	$2.324 \times 10^4$
$k_2^0$ (lit mol <sup>-1</sup> min <sup>-1</sup> )	$12.727 \times 10^8$

## Conclusion

The results of this study demonstrate that Box-Behnken design-based RSM could efficiently optimize the amberlite IR 120 and sulphamic acid-catalyzed esterification of methanol and acetic acid. The experimental investigation encompassed the examination of various factors, such as temperature, molar ratio of reactants and catalyst loading. The result shows that the amberlite IR 120 catalyst was better than the sulphamic acid catalyst due to the more active catalyst surface area. The conversion of acetic acid increases with temperature as well as molar ratio of reactants and catalyst loading. The experimental evidence indicates that as the temperature rises, the acetic acid conversion rate also escalates due to heightened energetic collisions facilitating the transition from reactant to product formation. Similarly, the catalyst loading (amberlite IR 120) exhibits a direct correlation with the provided mole ratio, resulting in an augmented transformation of acetic acid owing to the substantial presence of a large active surface area of catalyst. The kinetic data of the pseudo homogeneous model was utilized alongside the experimental findings conducted within the temperature range of 308.15 K to 330.15 K, with a 1:1 mole ratio of reactants. The amberlite IR 120 catalyzed reaction yielded forward and reverse reactions with respective activation energies of 10.64 kJ mol<sup>-1</sup> and 47.65 kJ mol<sup>-1</sup>.

## Acknowledgement

The Research is financially supported by the DST-SERB New Delhi.

## References

- Calvar N, González B, & Dominguez A, *Chem Eng Process.: Process Intensif*, 46 (2007) 1317.
- Sakhre V, *Distillation - Modelling, Simulation and Optimization*, (Intech Open, UK), 2019.
- Jagadeesh Babu P E, Sandesh K, M. B. & Saidutta M B, *Ind Eng Chem Res*, 50 (2011) 7155.
- Rudelstorfer G, Neubauer M, Siebenhofer M, Lux S & Grafshafter A, *Chemie Ingenieur Technik*, 94 (2022) 671.
- Mekala M & Goli V R, *Chin J Chem Eng*, 23 (2015) 100.
- Mekala M & Goli V R, *Data Brief*, 18 (2018) 947.
- Yang Z, Peng M, Li Y, Wu X, Gui T, Li Y, Zhang F, Chen X & Kita H, *Membranes*, 12 (2022) 1269.
- Mekala M & Goli V R, *Prog React Kinet Mech*, 40 (2015) 367.
- Kusuma H S, Ansori A & Mahfud M, *J Chem Tech Met*, 56 (2021) 686.
- Deka T J, Osman A I & Baruah D C, *Env Chem Lett*, 20 (2022) 3525.
- Biswal S, Das S R & Saha N, *Env Dev Sustain*, (2023). <https://doi.org/10.1007/s10668-023-03752-6>.
- Kvamme B, *Fluids*, 6 (2021) 345.
- Nagtode V S, Cardoza C, Yasin H K A, Mali S N, Tambe S M, Roy P, Singh K, Goel A, Amin P D, Thorat B R, Cruz J N & Pratap A P, *ACS Omega*, 24 (2023) 11674.
- Kibar M E, Hilal L, Çapa B T, Bahçivanlar B & Abdeljelil B, *Chem Bio Eng Rev*, 10 (2023) 412.
- Dawaymeh F, Elmutasim O, Gaber D, Gaber S, Reddy K S K, Basina G, Polychronopoulou K, Al-Wahedi Y & Karanikolos G N, *Mol Cat*, 501 (2021) 111371.
- Cole-Hamilton D J & Tooze R P, *Catalyst Separation, Recovery and Recycling*, Vol. 30, (Springer, Dordrecht), 2006, p. 1-8.
- Jyoti G, Keshav A, Anandkumar J & Bhoi S, *Int J Chem Kinet*, 50 (2018) 370.
- Wang B, Wang B, Shukla S K & Wang R, *Catalysts*, 13 (2023) 740.
- Brondani L N, Ribeiro J S & Castilhos F, *Renew Energy*, 156 (2020) 579.
- Kalakuntala R & Suranani S, *Mater Today Proc*, 47 (2021) 4814.

- 21 Lee C S, Vorwerk C, Azudin N Y, Ahmad N A & Shukor S R A, *J Env Chem Eng*, 9 (2021) 105219.
- 22 Draper N & John J A, *Technometrics*, 30 (1988) 423.
- 23 Körbahti B K, Aktas N & Tanyolac A, *J Hazard Mater*, 148 (2007) 83.
- 24 Amini M, Younesi H, Bahramifar N, Lorestani A A Z, Ghorbani F, Daneshi A & Sharifzadeh M, *J Hazard Mater*, 154 (2008) 694.
- 25 Rade L L, Lemos C O T, De Souza B M A, Ribas R M, Monteiro R S & Hori C E, *Renew Energy*, 131 (2019) 348.
- 26 Prasertpong P, Jaroenkhasemmesuk C, Regalbutto J R, Lipp J & Tippayawong N, *Energy Rep*, 6 (2020) 1.
- 27 Balajii M & Niju S, *Biofuels*, 12 (2021) 495.
- 28 Punsuvon V, Nokkaew R, Somkliang P, Tapanwong M & Karnasuta S, *Energy Sources A Recovery Util Environ Eff*; 37 (2015) 846.
- 29 Gholivand S, Lasekan O & Tan C P, *Chem Cent J*, 11 (2017) 44.
- 30 Tiwari A, Keshav A & Bhowmick S, *Int J Chem Reactor Eng*, 15 (2017) 20160101.
- 31 Ghoshna J, Keshav A & AnandKumar J, *Ind J Chem Tech*, 26 (2019) 89.
- 32 Suryawanshi M A, Shinde N H & Nagotkar R V, *Int J Adv Res Sci Eng Technol*, 1 (2014) 17.